Comprehensive analysis of polarimetric radar cross-section parameters for insect body width and length estimation

Weidong LI[1,2], Cheng HU[1,2,3*], Rui WANG[1,2,3], Shaoyang KONG[3] & Fan ZHANG[3]

[1]*Radar Research Lab, School of Information and Electronics, Beijing Institute of Technology, Beijing* 100081, *China;*
[2]*Advanced Technology Research Institute, Beijing Institute of Technology, Jinan* 250300, *China;*
[3]*Key Laboratory of Electronic and Information Technology in Satellite Navigation*
(*Beijing Institute of Technology*), *Ministry of Education, Beijing* 100081, *China*

Abstract The length and width of insect body are critical parameters for entomological radar species identification. However, the body width is not measurable in entomological radar currently. In this study, the scattering matrices (SM) of 159 insect specimens were measured using an X-band fully polarimetric laboratory rig in a microwave anechoic chamber. The relationships between the polarimetric radar cross-section (RCS) parameters extracted from the SM and the insect body width were studied. It was found that all these parameters have good correlations with the body width and can be used to estimate it. The mopping relationships between the polarimetric RCS parameters and the body width are built, and can be used as empirical formulas for insect body width estimation. In addition, based on these parameters, two new body length estimation methods were proposed. The performance of the proposed body width and length estimation methods when the echo signals were noisy was analyzed. It was found that the parameter that represents the product of the RCSs when the polarization direction is parallel and perpendicular to the insect body axis has the best performance for both the estimation of body width and length.

Keywords insect, entomological radar, polarimetric RCS parameters, body width estimation, body length estimation

1 Introduction

Insect migration is one of the most important annual animal movements in terrestrial ecosystems [1]. Identifying and monitoring insect migration is crucial in managing pests and in assessing the effects of environmental change [2]. A traditional migratory insect monitoring tool is a suction trap that is set near a ground. This trap has been proven to be useful and important in the quantitative study of migratory insects. However, direct information about insect flight at altitudes above the trap cannot be obtained [2].

Radar is an important remote sensing tool that has been widely used for aerial target observation [3–5]. The ability of radar to detect high-flying insects without interfering with their flight makes it one of the most efficient tools for studying insect migration. Entomological radars have been used to study insect migration over half a century and provide an unparalleled opportunity to learn about the behavior of migrating insects [6]. In regard to the entomological radar, several migration phenomena such as dawn, morning, and dusk takeoffs; approximate downwind transport, concentration at wind convergences, layers in stable nighttime atmospheres, and nocturnal common orientation were obtained [7].

Identifying the insect targets detected with the entomological radar would improve the application of its observations in pest forecasting. Scanning radar was the earliest entomological radar employed to measure vertical density profile and common orientation of the migrating insect swarm. However,

---

scanning entomological radar can not identify species [8]. The X-band vertical-looking entomological radar (VLR) has been widely used since the 1990s. It employs a vertical beam that incorporates both rotating polarization and beam nutation [9, 10]. With this configuration, the VLRs are capable of measuring the speed, displacement direction, orientation, mass, wing-beat frequency, and shape parameters of the individual insect aloft [11, 12]. The biological parameters describing the insects (such as mass, wing-beat frequency, body length and width) and shape parameters of polarization are essential for species identification [13]. Owing to numerous moth species, many insects have similar biological and shape parameters. Thus, only rather broad classes can be recognized by VLR, and these will in consequence be relatively few in number [14, 15]. Measuring more biological parameters, such as body length and width (maximal abdomen width), improves the ability of species identification.

When measuring biological parameters, it is assumed that the insect is upright and horizontal, as well as illuminated directly below [12, 16]. The rotating linear polarization of the VLR allows the insect's polarization pattern, the variation of the radar cross-section (RCS) with the direction of linear polarization, to be measured [14, 17]. Based on the polarization pattern, the insect's polarimetric RCS parameters (a_0, a_1 and a_2) can be retrieved. The parameter a_0 is the average of the RCS over the total polarization angles (360°); a_1 and a_2 represent an elongated (a_1) and a cruciform (a_2) component of the polarization pattern, respectively. In addition, $\alpha_2 = a_1/a_0$ is introduced, which represents the effective shape of the polarization pattern [16]. With the assumption that the insect RCS was proportional to the target body mass in the X-band (i.e., the scattering of insects in the X-band is in the Rayleigh or the beginning of the resonance region), the polarimetric RCS parameters were used to estimate the mass of the insect [16–18]. Based on the measured insect RCS and mass (40–4000 mg) data, Aldhous discovered that a_0 can be used to construct a good insect mass estimator. Through parabola fitting, the first empirical equation of the insect mass is estimated [17]. In accordance with larger datasets of laboratory data on mass and RCS, Chapman improved the aforementioned method [18]. These empirical relationships are accurate within a factor of 2 for insect masses ranging from 1 mg to 3 g [19]. Based on 156 insect specimens, Drake improved the mass-RCS relationship by undertaking a multiple-regression analysis with insect mass as the dependent variable, and a_0 and α_2 as the independent variables. This new relationship yielded a 40% uncertainty in the mass estimates [16]. The most recent work, based on the insect scattering matrix (SM), indicates that the polarimetric RCS parameters ν (representing the RCS when the polarization direction is at right angles to the body axis) and d (representing the product of the RCSs when the polarization direction is parallel and perpendicular to the body axis) can be used to estimate insect mass with better performance [20]. The average relative errors of the masses retrieved from ν and d were 33.7% and 35.6%, respectively. Moreover, it was found that the parameters ν and d can be used to estimate the insect body length, with an average relative error of 20.0% and 22.7%, respectively. Note that no method has been proposed to estimate the body width from the radar parameters. Furthermore, the traditional polarimetric RCS parameters a_0, and a_0 & α_2 were only used for mass estimation. Because the body length and mass of an insect are strongly correlated, similar to ν and d, the polarimetric RCS parameters a_0, a_0 & α_2 may also be used to estimate insect body length.

Currently, polarimetric radar has been used in migratory insect research, and demonstrates strong class identification and parameter estimation capabilities. For large-scale migratory insect observation, in reference to polarization information, polarimetric weather radar can distinguish insects from birds, and identify whether the insect bodies are inclined [21, 22]. For individual insect target measurements, it has been validated that the insect's orientation, mass, and body length can be accurately extracted from the SM [20, 23, 24]. Based on the polarization and phase information of the SM, the lingering issue of parallel (PA) and perpendicular (PE) insect discrimination in radar entomology was resolved [25]. The target echo information measured by the fully polarimetric radar is represented by SM, which contains the backscattering signal amplitudes, as well as the phases and polarization information of a target. Note that since the polarization pattern measured by the VLR is uniquely determined by the SM and can be derived from it, the target information contained in the insect polarization pattern can be derived from the SM [20, 25]. However, the information contained in the SM (such as the phases and polarization information of a target) may not be derived from the polarization pattern. Therefore, a fully polarimetric system is expected to be adopted by the next-generation entomological radar. For a fully polarimetric entomological radar, SM-based insect parameter extraction should be adopted.

In this study, we demonstrate how the polarimetric RCS parameters can be obtained from an insect SM. The SMs of 159 insect specimens were measured through a fully polarimetric laboratory rig that was built with a four-port vector network analyzer and two X-band dual-polarized horn antennas. Based on

the measured insect SMs, the relationships between the body width and polarimetric RCS parameters a_0, a_0 & α_2, ν, and d were studied. The relationships between insect body length and the traditional polarimetric RCS parameters, a_0, and a_0 & α_2 were analyzed. It was found that all these parameters can be used to estimate the body width and length of the insects. To find the ideal parameter for body width and length estimation, the performances of these methods for different body-size insects and signal-to-noise (SNR) levels were analyzed.

2 Polarimetric RCS parameter calculation

In this section, we extract the polarimetric RCS parameters a_0, a_0 & α_2, ν, and d from the insect SM. Further details are elaborated in [17, 20].

The SM measured by the fully polarimetric radar can be written as

$$S = \begin{bmatrix} s_{11} & s_{12}e^{j\beta} \\ s_{21}e^{j\beta'} & s_{22}e^{j\gamma} \end{bmatrix}, \tag{1}$$

where s_{11}, s_{12}, s_{21}, and s_{22} represent the amplitude of each element, respectively; and, β, β', and γ represent the phases. For monostatic radars, $s_{12} = s_{21}$ and $\beta = \beta'$.

The parameters ν and d are invariant target parameters of the insect SM and are calculated from the eigenvalues of the Graves power matrix derived from the SM [20]. The Graves power matrix is defined as

$$G = S^{H}S = \begin{bmatrix} g_{11} & g_{12} \\ g_{21} & g_{22} \end{bmatrix}. \tag{2}$$

Here, the superscript H indicates the combined conjugate and transpose operations. Assuming $\lambda_1 \geqslant \lambda_2$, two eigenvalues of G can be represented as

$$\lambda_1 = \frac{(g_{11} + g_{22}) + \sqrt{(g_{11} - g_{22})^2 + 4g_{12}g_{21}}}{2}, \tag{3}$$

$$\lambda_2 = \frac{(g_{11} + g_{22}) - \sqrt{(g_{11} - g_{22})^2 + 4g_{12}g_{21}}}{2}, \tag{4}$$

where

$$\begin{cases} g_{11} = s_{11}^2 + s_{12}^2, \\ g_{12} = s_{11}s_{12}e^{j\beta} + s_{12}s_{22}e^{j(\gamma - \beta)}, \\ g_{21} = s_{11}s_{12}e^{-j\beta} + s_{12}s_{22}e^{-j(\gamma - \beta)}, \\ g_{22} = s_{12}^2 + s_{22}^2. \end{cases} \tag{5}$$

Based on λ_1 and λ_2, ν and d can be represented as

$$\nu = \begin{cases} \lambda_2, & \text{PA} \quad \text{insect,} \\ \lambda_1, & \text{PE} \quad \text{insect,} \end{cases} \tag{6}$$

$$d = \sqrt{\lambda_1\lambda_2}, \tag{7}$$

where PA and PE insects represent the insects whose maximal RCS of polarization pattern occurs when the polarization direction is parallel and perpendicular to the insect body axis, respectively [25]. ν represents the RCS when the polarization direction is at a right angle with the body axis. For the PA insect, λ_1 and λ_2 represent the RCSs when the polarization direction is parallel and perpendicular to the insect body axis, respectively. However, for PE insects, the physical meanings of λ_1 and λ_2 are exchanged. Thus, to obtain ν, discriminating the class (PA or PE) of insects is necessary. The relative phase $\Delta\phi$ of the SM eigenvalues provides useful discrimination [25]. The two eigenvalues of the insect SM, μ_1 and μ_2 (not λ_1 and λ_2 mentioned above) can be calculated from SM in regard to eigenvalue decomposition. Without loss of generality, we may assume that $|\mu_1| \geqslant |\mu_2|$, therefore they can be represented as

$$\mu_1 = \frac{1}{2}\left(s_{11} + s_{22}e^{j\gamma}\right) + \frac{1}{2}\sqrt{\left(s_{11} - s_{22}e^{j\gamma}\right)^2 + 4s_{12}s_{21}e^{j(\beta + \beta')}} = |\mu_1|e^{j\phi_1}, \tag{8}$$

$$\mu_2 = \frac{1}{2}\left(s_{11} + s_{22}\mathrm{e}^{\mathrm{j}\gamma}\right) - \frac{1}{2}\sqrt{\left(s_{11} - s_{22}\mathrm{e}^{\mathrm{j}\gamma}\right)^2 + 4s_{12}s_{21}\mathrm{e}^{\mathrm{j}(\beta+\beta')}} = |\mu_2|\,\mathrm{e}^{\mathrm{j}\phi_2}, \tag{9}$$

where $|\mu_1|$ and $|\mu_2|$ indicate the amplitudes of μ_1 and μ_2, respectively, and ϕ_1 and ϕ_2 represent their phases. The relative phase $\Delta\phi$ is defined as follows:

$$\Delta\phi = \phi_1 - \phi_2 + 2k\pi, \quad \Delta\phi \in (-\pi, \pi], \quad k = 0, \pm 1, \tag{10}$$

where ϕ_1 and $\phi_2 \in (-\pi, \pi]$; $2k\pi$ is introduced to make $\Delta\phi \in (-\pi, \pi]$.

Based on the property that the sign of $\Delta\phi$ is always negative for the PA insect and positive for the PE insect, PA and PE insects can be discriminated [25]

$$\text{Insect class} = \begin{cases} \text{PA} & \text{insect}, \quad \Delta\phi < 0, \\ \text{PE} & \text{insect}, \quad \Delta\phi > 0. \end{cases} \tag{11}$$

Therefore, Eq. (6) can be updated as

$$\nu = \begin{cases} \lambda_2, & \Delta\phi < 0, \\ \lambda_1, & \Delta\phi > 0. \end{cases} \tag{12}$$

The traditional VLR is rotating linear polarization configuration that measures the insect's polarization pattern. For VLRs, the polarimetric RCS parameters a_0 and α_2 were estimated from the polarization pattern based on an estimation algorithm, such as the least squares estimation. The polarization pattern can be represented as

$$\sigma(\alpha) = a_0 + a_1\cos 2(\alpha - \theta_1) + a_2\cos 4(\alpha - \theta_2), \tag{13}$$

where α represents the direction of linear polarization; a_0 is the average of the RCS over all polarization angles ($360°$), a_1 and a_2 are magnitudes of harmonic modulations representing an elongated (a_1) and a cruciform (a_2) component, and θ_1 is the orientation of the insect.

Similar to ν, α_2 is an insect-class dependence parameter, and $\Delta\phi$ is required for insect class discrimination. α_2 can be represented as

$$\alpha_2 = \begin{cases} \dfrac{a_1}{a_0}, & \Delta\phi < 0, \\ -\dfrac{a_1}{a_0}, & \Delta\phi > 0. \end{cases} \tag{14}$$

To calculate a_0 and α_2 from the SM, the polarization pattern should be represented with the SM, which can be written as [17]

$$\sigma(\alpha) = \left| [\cos\alpha \ \sin\alpha]\, \boldsymbol{S} \begin{bmatrix} \cos\alpha \\ \sin\alpha \end{bmatrix} \right|^2. \tag{15}$$

Equating Eqs. (13) and (15), we obtain

$$a_0 = \frac{1}{8}\left(3s_{11}^2 + 3s_{22}^2 + 4s_{12}^2 + 2s_{11}s_{12}\cos\gamma\right), \tag{16}$$

$$\alpha_2 = \begin{cases} \dfrac{\sqrt{a_{11}^2 + a_{12}^2}}{a_0}, & \Delta\phi < 0, \\ -\dfrac{\sqrt{a_{11}^2 + a_{12}^2}}{a_0}, & \Delta\phi > 0, \end{cases} \tag{17}$$

where

$$\begin{cases} a_{11} = \dfrac{1}{2}\left(s_{11}^2 - s_{22}^2\right), \\ a_{12} = s_{12}\left[s_{11}\cos\beta + s_{22}\cos(\beta - \gamma)\right]. \end{cases} \tag{18}$$

Hitherto, all polarimetric RCS parameters can be calculated from the insect SM.
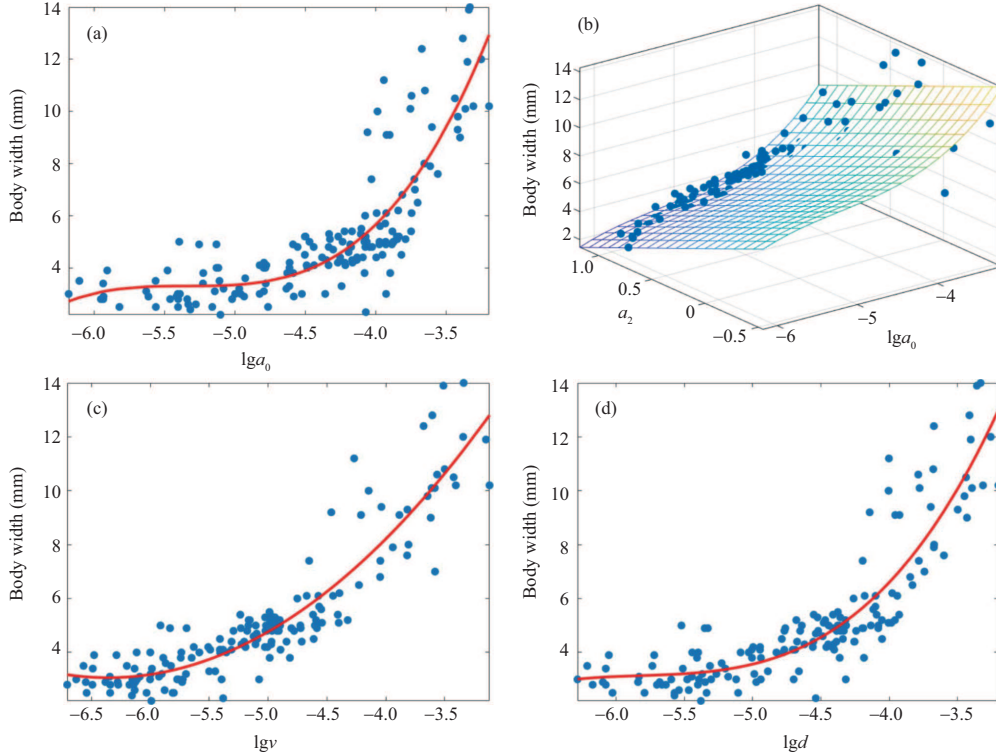
Figure 1 (Color online) Relations of insect body widths to polarimetric RCS parameters: (a) a_0; (b) a_0 & α_2; (c) ν; (d) d. The dots represent the 159 insect specimens. The curves and the wireframe mesh represent the fits to body widths.

3 Body width and length estimation

3.1 Experiment data

The insect SM measurements were made using a fully polarimetric rig in a microwave anechoic chamber. This rig was mainly constructed using a four-port vector network analyzer and 2 dual-polarized X-band horn antennas (one for transmitting and the other for receiving). The rig was able to measure 4 different polarization echoes (HH, HV, VH, VV) of insects. The vector network analyzer could be used to measure RCS precisely, which has been applied for insect and bat RCS measurements [23, 26]. In this study, the center frequency was set to 9.4 GHz and the bandwidth was 500 MHz. The insects were upright and horizontal. The antennas were mounted directly below to illuminate the insect at the near-ventral aspect. A hollow steel ball with a diameter of 32.2 mm was measured simultaneously, providing polarization and RCS calibrations.

In the measurement, 159 specimens representing 23 different species were measured. Their masses ranged from 20.2 to 964 mg, body lengths from 10.3 to 47 mm, and body widths from 2.2 to 14 mm. Most of the measured specimens were PA insects (151 specimens); only 8 specimens were PE insects. The parameters a_0, a_0 & α_2, ν, and d were extracted from the SMs of the measured 159 specimens to study the relationships between body length and width and polarimetric RCS parameters.

3.2 Body width estimation

Reportedly, all these polarimetric RCS parameters a_0, a_0 & α_2, ν and d can be used to estimate the insect mass. Additionally, the parameters ν and d can be used to estimate insect body length. In this subsection, we study whether these parameters can be used to estimate insect body width. The relationships between the body widths and the parameters a_0, a_0 & α_2, ν and d are presented as scatter diagrams in Figure 1. We can observe that all these parameters are strongly correlated with body width. The mapping relationships between body width and polarimetric RCS parameters can be described using mathematical equations, which can be used as empirical equations to estimate insect body width.

The empirical formulas for body width estimation can be obtained from the data by fitting. For single-parameter methods, the insect body widths can be fitted with the polynomials in logarithm-transformed
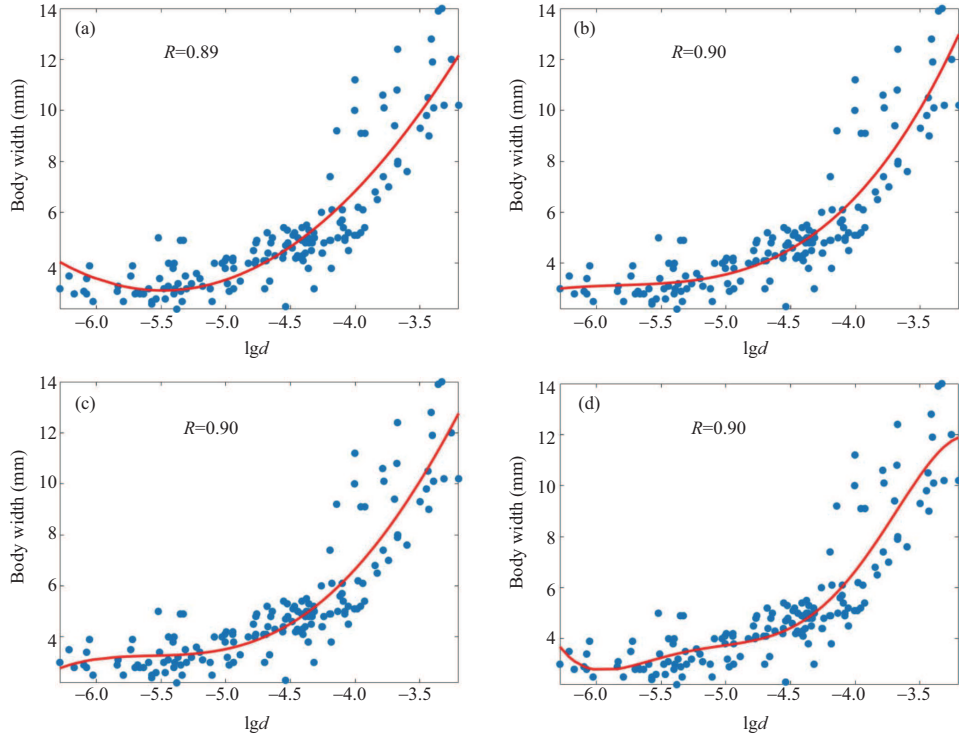
Figure 2   (Color online) The fitted insect body widths and $\lg d$ with different order polynomials: (a) 2nd-order; (b) 3rd-order; (c) 4th-order; (d) 5th-order. The dots represent the 159 insect specimens. The curves are the fitting results.

a_0, ν and d, respectively. For the parameter-pair method, the insect body widths can be fitted with the regression analysis in α_2 and $\lg a_0$. Selecting a proper order for fitting is important. If the fitting order is too low, under-fitting can easily occur, and the correlation coefficient (R) between the fitting curve and the true value will be small. If the fitting order is too high, R will be large, but over-fitting can easily occur. Therefore, the desired order maximizes R and avoids under- and over-fitting. To show how to determine the fitting order, the insect body widths were fitted with different order (2nd–5th) polynomials in $\lg d$, as shown in Figure 2. It can be observed that the 2nd-order fitting curve is under-fitting for the small insects (Figure 2(a), lower left). The 5th-order fitting curve (Figure 2(d)) is over-fitting. The R and the curves of the 3rd and 4th-order fitting results (Figure 2(b) and (c)) are similar. It seems that both the 3rd and 4th-order fitting curves are ideal. In this case, the lower order assumes precedence. Thus, the 3rd-order fitting curve is selected.

Based on the above method, the fitting orders of these parameters were determined. The best fitting orders of the single parameter methods $\lg a_0$, $\lg \nu$ and $\lg d$ are all 3rd. For the parameter-pair method, the fitting orders of $\lg a_0$ and α_2 are 3rd and 1st, respectively. The fitting results are shown as curves and the wireframe mesh in Figure 1. These fitted curves or curve surface can be represented as

$$W_{a_0} = 0.9721 \cdot [\lg a_0]^3 + 15.5770 \cdot [\lg a_0]^2 + 83.2178 \cdot [\lg a_0] + 151.5163, \tag{19}$$

$$W_{a_0 \& \alpha_2} = 0.5058 \cdot [\lg a_0]^3 + 7.9168 \cdot [\lg a_0]^2 + 42.1271 \cdot [\lg a_0] - 3.3436 \cdot [\lg \alpha_2] + 82.7251, \tag{20}$$

$$W_\nu = 0.0025 \cdot [\lg \nu]^3 + 0.9668 \cdot [\lg \nu]^2 + 11.9944 \cdot [\lg \nu] + 40.8812, \tag{21}$$

$$W_d = 0.5251 \cdot [\lg d]^3 + 9.1658 \cdot [\lg d]^2 + 53.4946 \cdot [\lg d] + 107.5346. \tag{22}$$

The above equations can be used as empirical formulas to estimate insect body widths in millimeters.

The fitting methods, correlation coefficients R, and mean relative errors (MRE) of these parameters are listed in Table 1. MRE is used to evaluate the accuracy of the estimates, which is defined as

$$\mathrm{MRE} = \mathrm{E}\left(\left|\frac{\text{Estimated value} - \text{True value}}{\text{True value}}\right| \times 100\%\right), \tag{23}$$

where $\mathrm{E}(\cdot)$ represents the mean value operation. It can be seen that the ν and a_0 & α_2 methods have similar good performance (ν: $R = 0.92$ and $\mathrm{MRE} = 13.25\%$; a_0 & α_2: $R = 0.92$ and $\mathrm{MRE} = 13.32\%$).

Table 1 Comparison of polarimetric RCS parameters for insect body width estimation

Parameter	Fitting method	$R^{a)}$ (P value[b)])	MRE (%)
ν	3rd-order polynomial	0.92 ($P < 0.001$)	13.25
d	3rd-order polynomial	0.90 ($P < 0.001$)	15.53
a_0	3rd-order polynomial	0.86 ($P < 0.001$)	18.16
a_0 & α_2	Regression analysis	0.92 ($P < 0.001$)	13.32

[a)] Pearson correlation coefficient, evaluating the correlation between the fitted and the true values.
[b)] P value is used to test the null hypothesis of no correlation. A value less than 0.001 provides strong evidence for a correlation.
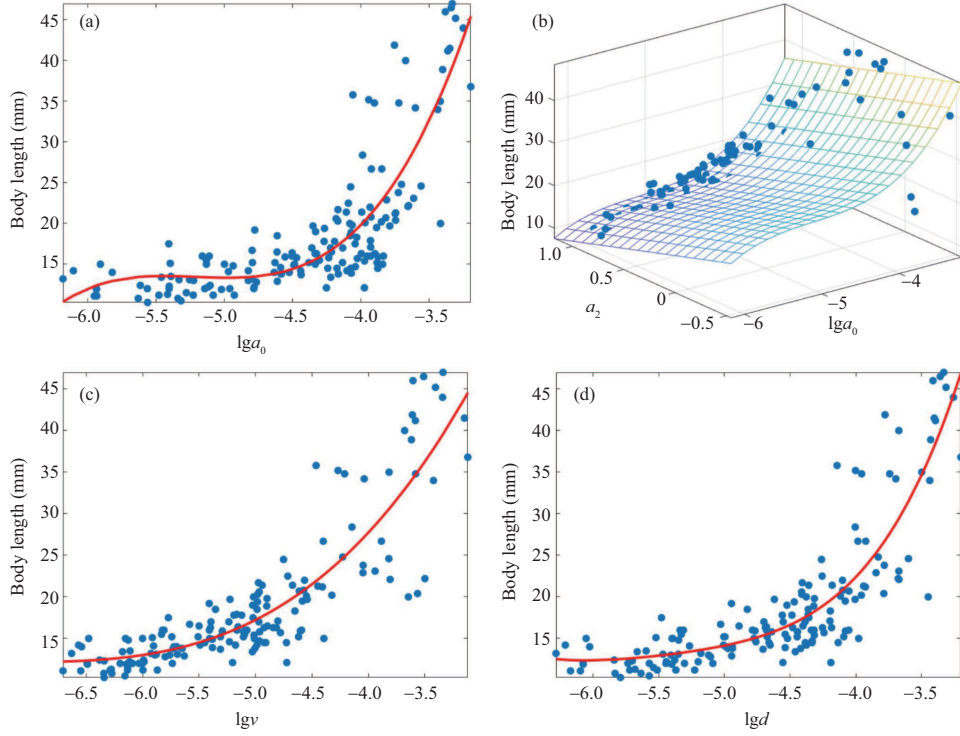

Figure 3 (Color online) Relations of insect body lengths to polarimetric RCS parameters: (a) a_0; (b) a_0 & α_2; (c) ν; (d) d. The dots represent the 159 insect specimens. The curves and the wireframe mesh represent the fits to body lengths.

The d method followed ($R = 0.90$ and MRE $= 15.53\%$). The a_0 method has a correlation coefficient R of 0.86 and MRE of 18.16%.

3.3 Body length estimation

We note that the traditional polarimetric RCS parameters a_0, and a_0 & α_2 were only used for mass estimation. As the body length and mass of an insect are strongly correlated, similar to ν and d, the parameters a_0, and a_0 & α_2 may also be used to estimate insect body length. To verify this, the relationships between the body lengths and parameters a_0, and a_0 & α_2 are studied, which are shown as scatter diagrams in Figure 3(a) and (b), respectively. It can be observed that a_0, and a_0 & α_2 are strongly correlated with body length, and therefore, can be used to estimate the insect body length.

For comparison, the ν and d methods are refitted based on our sample. The best fitting curves of single-parameter methods $\lg a_0$, $\lg \nu$, and $\lg d$ for body length fitting are all 3rd-orders. For the parameter-pair method, the fitting orders of $\lg a_0$ and α_2 are 3rd and 1st, respectively. The fitted results are presented in Figure 3. These fitted curves and curved surfaces can be represented as

$$L_{a_0} = 4.0756 \cdot [\lg a_0]^3 + 63.7101 \cdot [\lg a_0]^2 + 331.2836 \cdot [\lg a_0] + 586.4569, \tag{24}$$

$$L_{a_0 \& \alpha_2} = 3.034 \cdot [\lg a_0]^3 + 46.5950 \cdot [\lg a_0]^2 + 239.4741 \cdot [\lg a_0] - 7.4706 \cdot [\lg \alpha_2] + 432.756, \tag{25}$$

$$L_\nu = 0.4883 \cdot [\lg \nu]^3 + 10.4644 \cdot [\lg \nu]^2 + 74.8990 \cdot [\lg \nu] + 191.1580, \tag{26}$$

$$L_d = 2.6412 \cdot [\lg d]^3 + 43.3021 \cdot [\lg d]^2 + 237.4036 \cdot [\lg d] + 448.5243, \tag{27}$$

Table 2 Comparison of polarimetric RCS parameters for insect body length estimation

Parameter	Fitting method	R (P value)	MRE (%)
ν	3rd-order polynomial	0.88 ($P < 0.001$)	13.53
d	3rd-order polynomial	0.88 ($P < 0.001$)	14.30
a_0	3rd-order polynomial	0.85 ($P < 0.001$)	16.07
a_0 & α_2	Regression analysis	0.87 ($P < 0.001$)	14.18
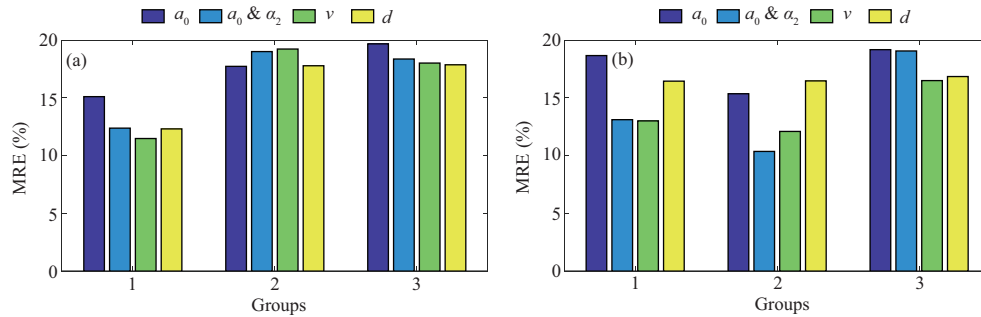
Figure 4 (Color online) Performances comparison of a_0, a_0 & α_2, ν and d methods for different body size samples: (a) body length estimation; (b) body width estimation.

The above equations can be used as empirical formulas to estimate insect body lengths in millimeters.

The fitting methods, R and MRE, between the fitted and the true values of the insect body lengths are listed in Table 2. The ν method has the best performance($R = 0.88$, MRE $= 13.53\%$), and is slightly better than the d ($R = 0.88$ and MRE $= 14.30\%$) and a_0 & α_2 ($R = 0.87$ and MRE $= 14.18\%$) methods. These three methods have comparably good performance. On the other hand, a_0 has correlation coefficient R of 0.85, and MRE of 16.07%.

3.4 Performance analysis

All these polarimetric RCS parameters can be used to estimate insect body width and length. The performances of these methods were compared.

3.4.1 *Performance for different body size insects*

Based on their body lengths, the 159 insect specimens were divided into 3 groups: the small insect, the middle insect, and the large insect, whose body lengths were in the ranges 10–20 mm, 20–30 mm, and 30–47 mm, respectively. The sample sizes of the groups were 114, 27, and 18, respectively. The performances of the four methods for the groups for the body length and width estimations are shown in Figure 4(a) and (b), respectively.

For body length estimation, the a_0 method has good performance for the middle insects, but has much poorer performance for the small and large insects as shown in Figure 4(a). The performances of the ν, d and a_0 & α_2 methods are similar for all the 3 insect groups. The ν method performs slightly better for small insects. The d method performed well for the middle insects. Furthermore, the MRE of the small insects is smaller than that of the middle and large insects.

For body width estimation, it can be seen from Figure 4(b) that for the small insects, the ν and the a_0 & α_2 methods have the closest and best performance. For the middle insects, the a_0 & α_2 method performs best; then, the ν method follows closely; the d method is close to the a_0 method. For large insects, the ν method has the best performance, followed by the d method; the a_0, and a_0 & α_2 methods have the closest but worst performances. Therefore, the ν method has the robust good performance for all the insects; the a_0 & α_2 method has good performance for the small and middle insects; the d method only has good performance for the large insects; the a_0 method has the poorest performance for all the three insect groups. Moreover, these methods have better performance for small and middle insects than for large insects.
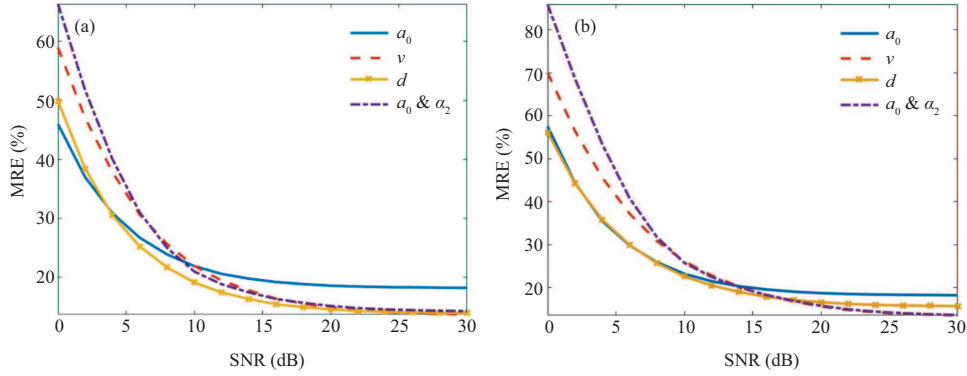
Figure 5 (Color online) Relationships between MRE and SNR for (a) body length estimation; (b) body width estimation.

3.4.2 *Performance at different SNR levels*

The insect data used in this study were measured in the laboratory and their SNRs for the measurement were high (most were greater than 30 dB). However, the SNR of the flying insects could be low in the real case. Thus, it is necessary to evaluate the performance of these methods at different SNR levels. Since the fully polarimetric radar measures the elements of the SM, the noise directly affects the SM. Thus, the measured SM can be modeled as

$$\boldsymbol{S}_m = \boldsymbol{S} + \boldsymbol{N}, \tag{28}$$

where $\boldsymbol{S}$ is the target SM and $\boldsymbol{N}$ is the complex white Gaussian noise matrix. It was assumed that the mean noise levels of the 4 polarization channels (HH, HV, VH, VV) are equal. Thus, the SNRs of the 4 channels could be different, because the 4 elements of the SM are different. In this study, the SNR is calculated as the level of the HH signal divided by the mean noise level.

To evaluate the performance of these methods for estimating body length and width when the echo signals were noisy, additional simulated noises were added to the measurement data and the polarimetric RCS parameters were recalculated. Based on the empirical formulas, the body lengths and widths of the specimens were estimated, and the corresponding MREs were calculated. The relationships between MREs and SNRs for body length and width estimation are shown in Figure 5(a) and (b), respectively.

For the body length estimation, the MRE decreases as the SNR increases for all four methods as shown in Figure 5(a). When the SNR is less than 9 dB, the a_0 and d methods exhibit comparably good performance; the a_0 & α_2 method has the worst performance, followed by the ν method closely. However, when the SNR is larger than 9 dB, the performances of the ν and a_0 & α_2 methods gradually approach that of the d method, and they all have small MREs (towards 14%), but the a_0 method has the worst performance (towards 18%). Therefore, the ν and a_0 & α_2 methods perform poorly at low SNR but well at high SNR; on the contrarily, the a_0 method has good performance at low SNR but exhibits poor performance at high SNR; however, the d method performs well at both the low and high SNRs.

For the body width estimation, it can be seen from Figure 5(b) that the performances of these methods are similar to those for body length estimation, except that the d method is slightly worse than the ν and a_0 & α_2 methods when the SNR is higher than 18 dB.

4 Discussion

When the noise is not considered, the ν, d, and a_0 & α_2 methods have comparably good performances for body length estimation; for the width estimation, the ν and a_0 & α_2 methods still perform well, but the d method performs slightly worse. The a_0 method performs poorly in estimating for both the body length and width. When the insects are grouped by body size, it seems that the estimation accuracy of small insects is higher than that of large insects. For body length estimation, the performances of the ν, d, and a_0 & α_2 methods for different insect groups are similar; for body width estimation, the a_0 & α_2 method has good performance for the small and middle insects; the d method has only good performance for the large insects; the ν method has robust good performance for all the insects.

When the echo signals are noisy, the ν and a_0 & α_2 methods still perform well at high SNR levels for body length and width estimation, but poor at low SNR levels; the d method, however, always performs

well regardless of the SNR level. In addition, the ν and a_0 & α_2 methods require target class discrimination when calculating ν and α_2. Although the PA and PE insects can be discriminated based on the relative phase $\Delta\phi$ with a high correct rate, some misclassification is inevitable, which may cause estimation errors. For comparison, the parameter d applies to insects of all classes with no initial classification stage. In conclusion, d may be the best choice for estimating body length and width.

For the traditional rotating-polarization entomological radar, what is measured is the variation of the insect echo signal with polarization direction, which can also be derived from the insect SM based on mathematical operations. In this study, the SMs of 159 insect specimens were directly measured through a fully polarimetric laboratory rig. The polarimetric RCS parameters were directly calculated from the SMs. The results of this study verify that the fully polarimetric radar can be used to measure the body size parameters of insects. Moreover, the fully polarimetric radar can measure the polarization and phase information of the target, which cannot be measured by the rotating-polarization entomological radar. For example, the relative phase $\Delta\phi$ measured by the fully polarimetric radar can be used for discrimination of PA and PE insects. However, $\Delta\phi$ cannot be measured by the current VLRs. In view of the good target recognition ability of the fully polarimetric radar, it has great potential to become the next generation entomological radar.

5 Conclusion

In this study, based on 159 insect specimens measured through a fully polarimetric laboratory rig, the relationships between the insect body widths and the polarimetric RCS parameters a_0, a_0 & α_2, ν and d were studied. It was found that all these parameters are highly correlated with body width and can be used for estimating body width. In addition, besides parameters ν and d, parameters a_0, and a_0 & α_2 can be used for estimating body length. The empirical formulas for body width and length estimation were obtained based on our insect specimens. The performances of these parameters for body width and length estimation are discussed. The ν and a_0 & α_2 have comparable good performances for both body length and width estimation, followed by the d method; a_0 has the worst performance. However, when the noise is considered, the d method has the best comprehensive performance for body length and width estimation.

References

1 Hu G, Lim K S, Horvitz N, et al. Mass seasonal bioflows of high-flying insect migrants. Science, 2016, 354: 1584–1587
2 Smith A D, Reynolds D R, Riley J R. The use of vertical-looking radar to continuously monitor the insect fauna flying at altitude over southern England. Bull Entomol Res, 2000, 90: 265–277
3 Hu C, Wang Y X, Wang R, et al. An improved radar detection and tracking method for small UAV under clutter environment. Sci China Inf Sci, 2019, 62: 029306
4 Cui K, Hu C, Wang R, et al. Deep-learning-based extraction of the animal migration patterns from weather radar images. Sci China Inf Sci, 2020, 63: 140304
5 Zhou C, Wang R, Hu C. Equivalent point estimation for small target groups tracking based on maximum group likelihood estimation. Sci China Inf Sci, 2020, 63: 189302
6 Drake V A, Reynolds D R. Radar Entomology: Observing Insect Flight and Migration. London: CABI, 2012
7 Chapman J W, Drake V A, Reynolds D R. Recent insights from radar studies of insect flight. Annu Rev Entomol, 2011, 56: 337–356
8 Long T, Hu C, Wang R, et al. Entomological radar overview: system and signal processing. IEEE Aerosp Electron Syst Mag, 2020, 35: 20–32
9 Drake A. Automatically operating radars for monitoring insect pest migrations. Insect Sci, 2002, 9: 27–39
10 Drake V A, Hatty S, Symons C, et al. Insect monitoring radar: maximizing performance and utility. Remote Sens, 2020, 12: 596
11 Hu C, Li W Q, Wang R, et al. Insect flight speed estimation analysis based on a full-polarization radar. Sci China Inf Sci, 2018, 61: 109306
12 Smith A D, Riley J R, Gregory R D. A method for routine monitoring of the aerial migration of insects by using a vertical-looking radar. Phil Trans R Soc Lond B, 1993, 340: 393–404
13 Hu C, Kong S Y, Wang R, et al. Identification of migratory insects from their physical features using a decision-tree support vector machine and its application to radar entomology. Sci Rep, 2018, 8: 5449
14 Drake V A. Distinguishing target classes in observations from vertically pointing entomological radars. Int J Remote Sens, 2016, 37: 3811–3835
15 Hao Z H, Drake V A, Taylor J R, et al. Insect target classes discerned from entomological radar data. Remote Sens, 2020, 12: 673
16 Drake V A, Chapman J W, Lim K S, et al. Ventral-aspect radar cross sections and polarization patterns of insects at X band and their relation to size and form. Int J Remote Sens, 2017, 38: 5022–5044

17 Aldhous A C. An investigation of the polarization dependence of insect radar cross sections at constant aspect. Dissertation for Ph.D. Degree. Cranfield: Cranfield Institute of Technology, 1989

18 Chapman J W, Smith A D, Woiwod I P, et al. Development of vertical-looking radar technology for monitoring insect migration. Comput Electron Agr, 2002, 35: 95–110

19 Hobbs S E, Aldhous A C. Insect ventral radar cross-section polarisation dependence measurements for radar entomology. IEEE Proc Radar Sonar Navig, 2006, 153: 502–508

20 Hu C, Li W D, Wang R, et al. Insect biological parameter estimation based on the invariant target parameters of the scattering matrix. IEEE Trans Geosci Remote Sens, 2019, 57: 6212–6225

21 Zrnic D S, Ryzhkov A V. Observations of insects and birds with a polarimetric radar. IEEE Trans Geosci Remote Sens, 1998, 36: 661–668

22 Melnikov V M, Istok M J, Westbrook J K. Asymmetric radar echo patterns from insects. J Atmos Ocean Tech, 2015, 32: 659–674

23 Hu C, Li W D, Wang R, et al. Accurate insect orientation extraction based on polarization scattering matrix estimation. IEEE Geosci Remote Sens Lett, 2017, 14: 1755–1759

24 Li W D, Hu C, Wang R, et al. Experimental validations of insect orientation extraction based on fully polarimetric measurement. J Eng, 2019, 21: 7954–7957

25 Hu C, Li W D, Wang R, et al. Discrimination of parallel and perpendicular insects based on relative phase of scattering matrix eigenvalues. IEEE Trans Geosci Remote, 2020. doi: 10.1109/TGRS.2019.2959622

26 Mirkovic D, Stepanian P M, Kelly J F, et al. Electromagnetic model reliably predicts radar scattering characteristics of airborne organisms. Sci Rep, 2016, 6: 35637